Opt Quant Electron (2015) 47:1671–1677
DOI 10.1007/s11082-014-0024-y

Dependence of dark current on carrier lifetime for InGaAs/InP avalanche photodiodes

Q. Y. Zeng · W. J. Wang · J. Wen · P. X. Xu · W. D. Hu · Q. Li · N. Li · W. Lu

Received: 25 February 2014 / Accepted: 15 September 2014 / Published online: 24 September 2014

Abstract Effects of carrier lifetime of all layers on the dark current have been studied for the separate-absorption-grading-charge-multiplication InGaAs/InP avalanche photodiodes (APDs). The results indicate that the remarkably increasing of the dark current at the punch-through voltage strongly depends on the carrier lifetime of InGaAs absorption layer. According to the simulation results, we can estimate the carrier lifetime of InGaAs absorption layer and InP multiplication layer to be about 100 ns and 20 ps for our fabricated device. And we can see that the dark current of APDs near the breakdown voltage is mainly dominated by the thermal generation–recombination current from the InGaAs absorption layer and trap-assisted-tunneling current from the InP multiplication layer.

Keywords InGaAs/InP avalanche photodiodes · Dark current · Carriers lifetime

1 Introduction

Avalanche photodiodes (APDs) have attracted great attention in recent years since they can be used as single photon detection in the field of quantum cryptography, photon-correlation spectroscopy and remote sensing (Hadfield 2009). Most papers are dedicated to improve the APDs' performance (Pellegrini et al. 2006; Acerbi et al. 2013; Wang et al. 2010) through

Q. Y. Zeng · W. J. Wang (✉) · J. Wen · W. D. Hu · Q. Li · N. Li · W. Lu
National Laboratory for Infrared Physics, Shanghai Institute of Technical Physics, Chinese Academy of Sciences, Shanghai 200083, China
e-mail: wangwj@mail.sitp.ac.cn

Q. Y. Zeng · J. Wen · P. X. Xu · Q. Li
University of Chinese Academy of Sciences, Beijing 100000, China

W. J. Wang
Synergetic Innovation Center of Quantum Information and Quantum Physics, University of Science and Technology of China, Hefei 230026, Anhui, China

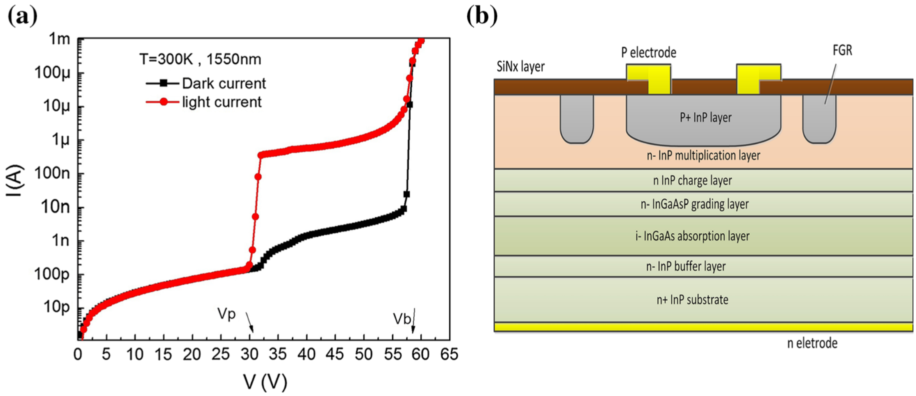

Fig. 1 **a** Current characteristic of experimental InGaAs/InP APDs at 300 K. **b** Cross section of the simulated APDs

the structure design, but few papers complain the reasons that lead to the poor performance, such as the high dark current.

For our fabricated separate-absorption-grading-charge-multiplication (SAGCM) InGaAs/InP APDs, we found that the dark current grows dramatically at the punch-through voltage (V_p), as shown in Fig. 1a. The dark current rises about 10 times (from 0.1 to 1 nA) when the bias is above V_p, and the increment can be suppressed by lowering the device temperature to 240 K, which indicates that this part of dark current is mainly composed of the thermally driven generation–recombination (G-R) current (Itzler et al. 2011; Zhao et al. 2011). The high G-R current means a high density of defects, which will influence the dark current near the breakdown voltage (V_b) and severely influence the performance of single photon detection. For the single photon detector operated in Geiger mode, the dominant dark current contains tunnneling current, which can be band-to-band or trap assited, and thermally driven G-R current (Itzler et al. 2008). The defects influence can be characterized by the minority carrier lifetime (Jiang et al. 2007). So, in this paper, we will discuss the effects of carrier lifetime on the dark current for every layer of the ASGCM InGaAs/InP APD.

2 Device structure and simulation model

Figure 1b is the schematic cross-section structure of a planar SAGCM InGaAs/InP APD. The n InP buffer layer was grown on the n^+ InP substrate, followed by an i-InGaAs absorption layer. Several InGaAsP layers with graded composition were then inserted between the absorption layer and n^- InP charge layer to avoid the hole accumulation which was caused by the valence band offset at InGaAs/InP heterojunction (Forrest et al. 1982). Adjacent to the n^- InP charge layer, an i-InP multiplication layer and a p+InP layer were fabricated sequentially. The internal electric field distribution in absorption layer and multiplication layer was adjusted by the thickness and doping concentration of the n-InP charge layer. The p^+ InP layer and the floating guard ring (FGR) structure were made by Zinc diffusion. For simplicity, thickness of the p^+ InP layer and the FGR are defined the same. Table 1 shows the structure parameters of the simulated InGaAs/InP APDs.

The two-dimensional numerical calculations were performed using Sentaurus software, a commercial package by Synopsys. The simulations are based on drift-diffusion

Table 1 Structure parameters of the simulated InGaAs/InP APDs

	InP-Sub	InP-buffer	InGaAs	InGaAsP	n-InP	i-InP	p+InP
Thickness (μm)	2.0	0.5	2.8	0.012 × 5	0.2	0.5	2.0
Doping (cm^{-3})	1e18	5e16	1e15	2e16	1e17	1e15	1e18

method, where the Poisson and continuity equations are coupled on the finite element mesh (D'Orsogna et al. 2008). The carrier G-R process consists of Shockley–Read–Hall (SRH), radiative, Auger, band-to-band tunneling (BBT), trap-assisted tunneling (TAT) and avalanche multiplication mechanisms. The TAT mechanism is incorporated into the SRH recombination rate, so the SRH recombination rate is (Shockley and Read 1952)

$$R_{SRH} = \frac{pn - n_i^2}{\frac{\tau_p}{1+\Gamma_p}\left[n + n_i \exp\left(\frac{E_t - E_i}{kT}\right)\right] + \frac{\tau_n}{1+\Gamma_n}\left[p + n_i \exp\left(\frac{E_i - E_t}{kT}\right)\right]} \quad (1)$$

here, n, p and n_i are the electron, hole, and the intrinsic carrier concentration, respectively. E_t is the trap energy level, k is the Boltzmann constant, T is the temperature, and τ is the carrier lifetime (p for holes, n for electrons). The TAT mechanism Γ is included by modify the SRH lifetime (Hall 1952). So the carrier lifetime mainly influence the thermal G-R current and TAT current.

3 Results and discussion

3.1 InP substrate and buffer layer, p+InP layer

The carrier lifetime of n-InP is in the range of 0–3,000 ns (Ahrenkiel 1991), depending on the crystal quality and the growth methods, while the carrier lifetime of p-InP is very short due to the high concentration of deep recombination centers and the dominance of non-radiative recombination (Rosenwaks et al. 1990). The largest effective lifetime of the n-InP (S-doped with majority carrier concentration $n_0 = 3 \times 10^{17} cm^{-3}$) is 110 ns, while it is below 1 ns for the p-InP (Zn-doped with majority carrier concentration $p_0 = 4 \times 10^{16} cm^{-3}$) (Liu and Rosenwaks 1999). And the lifetime decreases with the increasing of the doping concentration.

Figure 2a shows the dark current originated from the n^+ InP substrate and InP buffer layer. The carrier lifetime of other layers is set to 10 s so that only the specific layers are considered. We can see that the carrier lifetime only influences the dark current from the bias of 42 V, which is above the punch-through voltage (Vp = 32 V). The dark current increases remarkably with the bias untill it approaches the breakdown voltage (Vb = 57 V). The current increases from 5 fA to 1 pA when the carriers lifetime decreases from 50 ns to 100 ps at V = 46 V. Since the substrate and the buffer layer are not depleted before V = 42 V, the thermal G-R in these regions shows no contribution to the dark current, which also explains why the carrier lifetime of the p^+ InP layer has no influence on the dark current as shown in Fig. 2b. The doping concentration of the p^+ InP layer is set as 1×10^{18} cm^{-3}, so the depletion layer in p^+ InP is negligible. However, for the actual APDs, this depletion layer in p^+ InP layer is not negligible because the p^+ InP layer is formed by Zinc diffusion and the doping concentration distribution is gradient. We treat the depletion layer in p^+ InP as part of the multiplication layer (Wang et al. 2010; Zeng et al. 2013), just as the influence of carrier lifetime in n-InP multiplication layer.

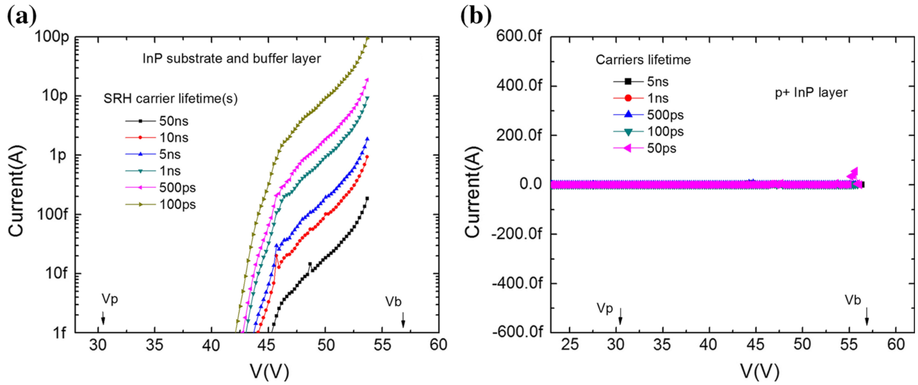

Fig. 2 **a** The dark current originated from the InP substrate and buffer layer. **b** The dark current originated from the p+InP layer

3.2 InGaAs absorption layer and InGaAsP grading layer

Gallant and Zemel (1988) (M. Gallant) measured the hole lifetime to be 18.5 μs in the undoped n-type InGaAs ($n_0 = 1 \times 10^{15}$ cm^{-3}), and the lifetime decreased with doping level because of a combination of radiative and Auger recombination (Henry et al. 1984; Ahrenkiel et al. 1998). On the other hand, the lifetime strongly depends on the growth techniques (Ehrlich et al. 1993). For example, the epitaxial growth may incorporate excess arsenic into the crystal in the form of point defects, which are associated with mid-gap trapping levels that can reduce the carrier lifetime to 500 fs (Baker et al. 2004). Besides, the carrier lifetime decreases distinctly with the decreasing of the layer growth temperature (Gupta et al. 1992). In addition, the annealing process may also introduce defects and influence the carrier lifetime.

Figure 3 shows the net dark current originated from the InGaAs absorption layer and InGaAsP grading layer, respectively. The dark current from InGaAs and InGaAsP layers both show remarkable increases near Vp, which is because the depletion region expands to the InGaAsP and InGaAs layers only when the bias is over Vp and the carrier lifetime of these layers only contributes to the dark current over Vp. We separate the dark current as thermal G-R current and TAT current. The thermal G-R current is larger than the TAT current even near the breakdown voltage since the electric filed in these layers is not strong. The thermal G-R dark current at V = 35 V increases from 100 pA to 10 nA with the carrier lifetime of InGaAs layer decreasing from 1 μs to 10 ns, while it increases from 5 to 500 pA for InGaAsP grading layer with the carrier lifetime decreasing from 100 to 1 ns. Because the thickness of the InGaAsP layer is negligible compared with the InGaAs layer, the thermal G-R current from InGaAsP layer is smaller than that from the InGaAs layer under the same condition. Compared with Fig.1a, the simulation is similar to our experimental results. According to Fig. 3a, we can estimate the carrier lifetime of the InGaAs layer in our fabricated devices to be about 100 ns.

3.3 InP charge layer and InP multiplication layer

Figure 4 shows the dark current originated from the InP charge layer and the InP multiplication layer. The TAT current completely dominates the dark current of InP charge layer and multiplication layer near the breakdown voltage, while the thermal G-R current mainly dom-

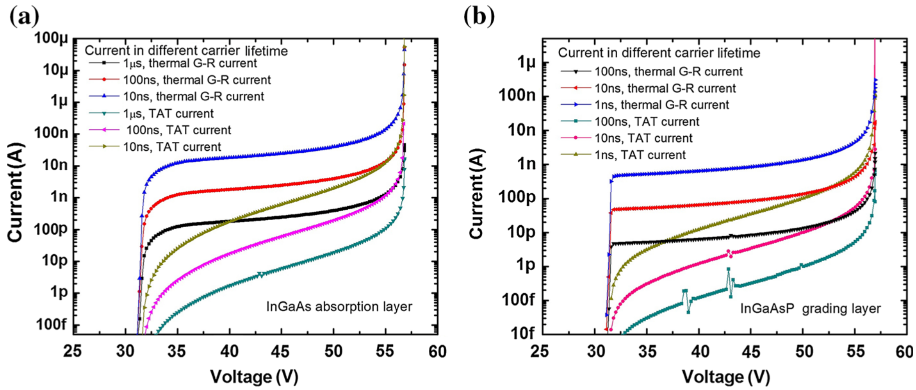

Fig. 3 **a** The dark current originated from the InGaAs absorption layer. **b** The dark current originated from InGaAsP grading layer

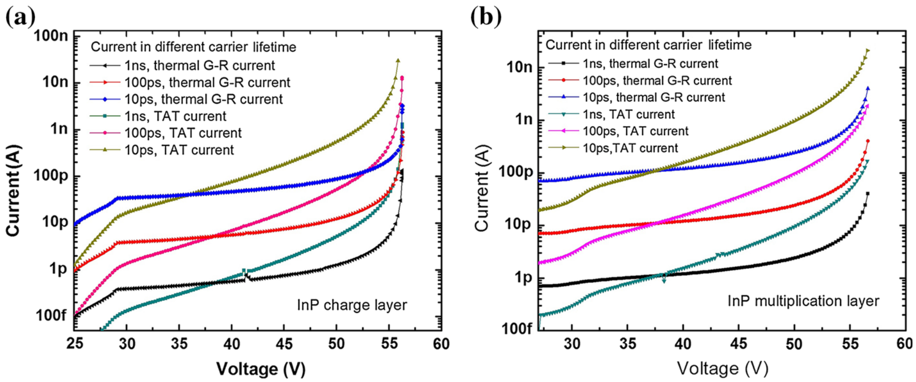

Fig. 4 **a** The dark current originated from the InP charge layer. **b** The dark current originated from the InP multiplication layer

inates the dark current near the punch-through voltage. The thermal G-R current at V = 32 V increases from about 15 pA to 1.3 nA with the carrier lifetime of InP charge layer decreasing from 100 to 1 ps. And it increases from 9 to 900 pA with the carrier lifetime of InP multiplication layer from 100 to 1 ps. Because the depletion region expands from the InP multiplication layer to the InP charge layer, InGaAsP grading layer, and then the InGaAs layer, so it's different from the InGaAs and InGaAsP layers that the carrier lifetime influences the dark current both below and above Vp. The electrical filed in the multiplication layer is so high that the electrons generated in the multiplication layer and charge layer can get sufficient energy to pass through the un-depletion zone in InGaAs absorption layer. And the holes can be collected easily by the p^+ InP layer since the device is reverse biased.

The charge layer is n-doped with the concentration of 1×10^{17} cm^{-3}, while the n-InP multiplication layer actually contains the depletion layer of p^+ InP, which is influenced by the Zinc diffusion and decreases the carrier lifetime of the multiplication layer. The carrier lifetime in the InP multiplication layer can be shorter than that of the InP charge layer. And, similar to the InGaAs absorption layer, we can estimate the carrier lifetime of multiplication layer in our fabricated device to be 10–50 ps at 300 K through the dark current at Vp (about 100 pA in the actual device).

Fig. 5 Components of the dark current in the SAGCM InGaAs/InP APDs

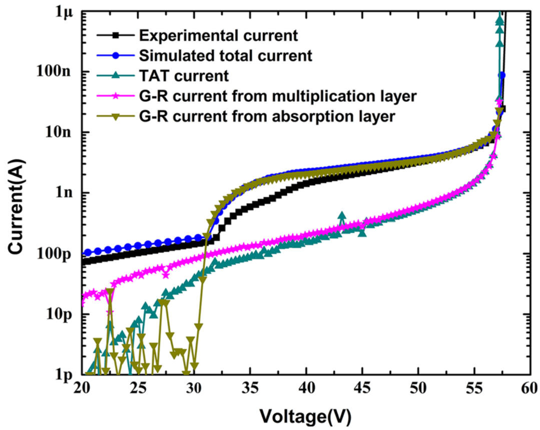

3.4 Simulation for experimental results

We simulate the dark current of APDs with appropriate carrier lifetime for our experimental device. The simulated results and the experimental dark current are shown in Fig. 5. The carrier lifetime of InGaAs absorption layer and InP multiplication layer are set as 100 ns and 20 ps, respectively. The simulated dark current fits well with the experiment results. It clearly shows that the dark current remarkably increasing at the punch-through voltage is mainly dominated by the thermal G-R current from the InGaAs absorption layer, and the dark current near the breakdown voltage is mainly due to the TAT current from the InP multiplcation layer and the thermal G-R current from the InGaAs absorption layer. For the fabricated device, defects in the thick InGaAs layer are not uniformly distributed, which results in the carrier lifetime is not constant in the InGaAs layer, so an obvious deviation of the experimental results from the simulation between 30–45 V is shown.

4 Conclusions

The dark current of the SAGCM InGaAs/InP APDs versus different carrier lifetime in all layers are studied in detail. The simulated results show that the carrier lifetime of the InP substrate and buffer layer only influence the dark current at V = 42 V above the punch-through voltage (Vp), and the carrier lifetime of InGaAs and InGaAsP layer influences the dark current just starting at Vp, while the carrier lifetime of the InP charge layer and multiplication layer contribute to dark current both below and above the punch-through voltage. The simulated results fit well with the experimental APDs, which indicates intuitively that the dark current rising in our experimental InGaAs/InP APDs near the punch-through voltage is coming from the InGaAs absorption layer. What's more, we can estimate roughly the carrier lifetime of the InGaAs layer and InP multiplication layer in our APDs to be about 100 ns and 20 ps. And the dark current of APDs near the breakdown voltage is mainly dominated by the thermal G-R current from the InGaAs absorption layer and trap-assisted-tunneling current from the InP multiplication layer. These results are useful for device's performance improvement.

Acknowledgments This work was supported by Strategic Pilot Program of Science and Technology of Chinese Academy of Sciences (XDB01010200), National Research Program of MOST (2011CB925600), National Natural Science Foundation of China (08K0510W15).

References

Acerbi, F., Anti, M., Tosi, A., Zappa, F.: Design criteria for InGaAs/InP single-photon avalanche diode. IEEE Photonics J. **5**, 6800209 (2013)

Ahrenkiel, R.K.: "Properties of InP", pp. 77. INSPEC, London. (1991)

Ahrenkiel, R.K., Ellingson, R., et al.: Recombination lifetime of $In_{0.53}Ga_{0.47}As$ as a function of doping density. Appl. Phys. Lett. **72**, 3470–3472 (1998)

Baker, C., Gregory, I.S., et al.: Highly resistive annealed low-temperature-grown InGaAs with sub-500fs carrier lifetimes. Appl. Phys. Lett. **85**, 4965–4967 (2004)

D'Orsogna, D., Tobin, S., et al.: Numerical analysis of a very long-wavelength HgCdTe pixel array for infrared detection. J. Electron. Mater. **37**, 1349–1355 (2008)

Ehrlich, J.E., Neilson, D.T., et al.: Carrier lifetimes in MBE and MOCVD InGaAs quantum wells. Semicond. Sci. Technol. **8**, 307–309 (1993)

Forrest, S.R., Kim, O.K., Smith, R.G.: Optical response time of In0.53Ga0.47As/InP avalanche photodiodes. Appl. Phys. Lett. **41**, 95–98 (1982)

Gallant, M., Zemel, A.: Long minority hole diffusion length and evidence for bulk radiative recombination limited lifetime in InP/InGaAs/InP double heterostructures. Appl. Phys. Lett. **52**, 1686–1688 (1988)

Gupta, S., Whitaker, J.F., Mourou, G.A.: Ultrafast carrier dynamics in III–V semiconductors grown by molecular-beam epitaxy at very low substrate temperatures. IEEE J. Quantum Electron. **28**, 2464–2472 (1992)

Hadfield, R.H.: Single-photon detectors for optical quantum information applications. Nat. Photonics **3**, 696–705 (2009)

Hall, R.N.: Electron-hole recombination in germanium. Phys. Rev. **87**, 387–387 (1952)

Henry, C.H., Logan, R.A., Merrit, F.R., Bethea, C.G.: Radiative and nonradiative lifetimes in n-type and p-type 1.6μm InGaAs. Electron. Lett. **20**, 358–359 (1984)

Itzler, M.A., Jiang, X.D., et al.: High-performance single photon avalanche diodes for QKD networks. In: SECOQC Conference 08 (2008)

Itzler, M.A., Jiang, X.D., et al.: Advances in InGaAsP-based avalanche diode single photo detectors. J. Modern Opt. **58**, 174–200 (2011)

Jiang, X., Itzler, M.A., Ben-Michael, R., Slomkowski, K.: InGaAs–InP avalanche photodiodes for single photon detection. IEEE Sel. Top. Quantum Electron. **13**, 895–905 (2007)

Liu, A., Rosenwaks, Y.: Excess carriers lifetime in InP single crystals: radiative versus nonradiative recombination. J. Appl. Phys. **86**, 430–437 (1999)

Pellegrini, S., Warburton, R.E., et al.: Design and performance of an InGaAs–InP single photon avalanche diode detector. IEEE J. Quantum Electron. **42**, 397–403 (2006)

Rosenwaks, Y., Shapira, Y., Huppert, D.: Metal reactivity effects on the surface recombination velocity at InP interfaces. Appl. Phys. Lett. **57**, 2552 (1990)

Shockley, W., Read, W.T.: Statistics of the recombinations of holes and electrons. Phys. Rev. **87**, 835–842 (1952)

Wang, W.J., Lin, L., et al.: Numerical analysis of single photon avalanche photodiodes with Improved structure. In: 10th International Conference on Numerical Simulation of Optoelectronic Devices, pp. 19–20 (2010)

Zeng, Q.Y., Wang, W.J., et al.: Numerical analysis of multiplication layer on dark current for InGaAs/InP single photon avalanche diodes'. Opt. Quant. Electron. (2013). doi:10.1007/s11082-013-9809-7

Zhao, Y., Zhang, D.: InGaAs–InP avalanche photodiodes with dark current limited by generation–recombination. Opt. Express **19**, 8546–8556 (2011)